Amplification of the gene for SCAP, coupled with Insig-1 deficiency, confers sterol resistance in mutant Chinese hamster ovary cells

Peter C. W. Lee,* Pingsheng Liu,† Wei-Ping Li,† and Russell A. DeBose-Boyd[1],*

Departments of Molecular Genetics* and Cell Biology,† University of Texas Southwestern Medical Center, Dallas, TX 75390-9046

Abstract The endoplasmic reticulum membrane proteins Insig-1 and Insig-2 limit cholesterol synthesis, in part through their sterol-dependent binding to sterol-regulatory element binding protein (SREBP) cleavage-activating protein (SCAP). This binding prevents proteolytic processing of SREBPs, membrane-bound transcription factors that enhance cholesterol synthesis. We report here the characterization of mutant Chinese hamster ovary (CHO) cells, designated SRD-19, that are resistant to 25-hydroxycholesterol, a potent inhibitor of SREBP processing. SRD-19 cells were produced by mutagenesis of Insig-1-deficient SRD-14 cells, followed by selection in high levels of 25-hydroxycholesterol. 25-Hydroxycholesterol fails to suppress SREBP processing in SRD-19, even though they express normal levels of Insig-2. The number of copies of the gene encoding SCAP was found to be increased by 4-fold in SRD-19 cells compared with wild-type CHO cells, leading to the overproduction of SCAP mRNA and protein. Our data indicate that overproduced SCAP saturates the remaining Insig-2 in SRD-19 cells, thus explaining their resistance to 25-hydroxycholesterol. Consistent with this conclusion, regulated SREBP processing is restored in SRD-19 cells upon transfection of plasmids encoding either Insig-1 or Insig-2. These results highlight the importance of SCAP/Insig ratios in normal sterol-regulated processing of SREBPs in cultured cells.—Lee, P. C. W., P. Liu, W-P. Li, and R. A. DeBose-Boyd. **Amplification of the gene for SCAP, coupled with Insig-1 deficiency, confers sterol resistance in mutant Chinese hamster ovary cells. *J. Lipid Res.* 2007.** 48: **1944–1954.**

Supplementary key words cholesterol homeostasis • endoplasmic reticulum-Golgi translocation • ubiquitination • somatic cell genetics • mutagenesis • sterol-sensing domain • sterol-regulatory element binding protein cleavage-activating protein

Sterol-induced retention of sterol-regulatory element binding protein (SREBP) cleavage-activating protein (SCAP) in the endoplasmic reticulum (ER) and sterol-accelerated degradation of ER-bound HMG-CoA reductase constitute two mechanisms by which animal cells limit the synthesis of cholesterol. Remarkably, both mechanisms are mediated by sterol-regulated binding of SCAP and reductase to polytopic ER membrane proteins called Insig-1 and Insig-2. In sterol-depleted cells, SCAP transports membrane-bound transcription factors called SREBPs from the ER to the Golgi, where the SREBPs are processed to forms that activate cholesterol synthesis (1). When cholesterol accumulates in ER membranes, the sterol binds to SCAP and this causes SCAP to bind Insigs (2–4). The Insig-bound SCAP-SREBP complex remains sequestered in ER membranes; levels of mRNAs encoding SREBP target genes decrease and the rate of cholesterol synthesis declines. HMG-CoA reductase catalyzes the conversion of HMG-CoA to mevalonate, a rate-controlling step in the synthesis of cholesterol and nonsterol isoprenoids (5). In sterol-depleted cells, the membrane-bound reductase is stable, with a half-life of >12 h. The accumulation of sterols in ER membranes triggers the binding of reductase to a subset of Insigs that carry a membrane-anchored ubiquitin ligase called gp78, which initiates reductase ubiquitination (6). This ubiquitination marks reductase for rapid, proteasome-mediated degradation, reducing the half-life of the protein to <1 h. The decrease in reductase reduces the production of mevalonate, hence blunting the rate of cholesterol synthesis. These two Insig-mediated events (ER retention of SCAP-SREBP and ubiquitination/degradation of reductase) are modulated to ensure a constant supply of substrates for the production of essential nonsterol isoprenoids while avoiding the overproduction of cholesterol or its sterol precursors.

SCAP and reductase share a similar topology in ER membranes. Each protein can be divided into two domains: a

Manuscript received 14 May 2007 and in revised form 20 June 2007.

Published, JLR Papers in Press, June 22, 2007.
DOI 10.1194/jlr.M700225-JLR200

Abbreviations: CHO, Chinese hamster ovary; ER, endoplasmic reticulum; SCAP, sterol-regulatory element binding protein cleavage-activating protein; SREBP, sterol-regulatory element binding protein.

[1] To whom correspondence should be addressed.
e-mail: russell.debose-boyd@utsouthwestern.edu

hydrophobic NH_2-terminal domain with eight membrane-spanning segments that anchor the proteins to ER membranes; and a large hydrophilic COOH-terminal domain that projects into the cytosol (7–9). The COOH-terminal domain of reductase exerts the enzyme's catalytic activity (10), whereas the COOH-terminal domain of SCAP mediates interactions with SREBPs (11). The membrane domains of both proteins are responsible for sterol-induced binding to Insigs (4, 12). The Insig binding site in SCAP and reductase localizes to an evolutionarily related intramembrane sequence called the sterol-sensing domain, which comprises transmembrane helices 2–6 of both proteins (13, 14). Point mutations within the sterol-sensing domains of SCAP and reductase prevent their association with Insigs, thereby abrogating sterol-mediated ER retention of SCAP-SREBP and sterol-induced ubiquitination/degradation of reductase (4, 15–17).

Previously, we described a genetic screen designed to isolate mutants of Chinese hamster ovary (CHO) cells that fail to degrade reductase upon addition of sterols (18). The screen was conducted by γ-irradiation of CHO cells, followed by selection in sterol-free medium supplemented with the 1,1-bisphosphonate ester SR-12813. SR-12813 blocks cholesterol synthesis by mimicking the action of sterols in accelerating the degradation of reductase. This screen gave rise to SRD-14 cells, which survived selection by virtue of an Insig-1 deficiency. However, SREBP processing in SRD-14 cells remained sensitive to 25-hydroxycholesterol, although the effect required extended exposure to the oxysterol compared with wild-type cells. We proposed that Insig-2, which accounts for 10% of total Insig in wild-type CHO cells, was sufficient to maintain this residual sterol regulation. To isolate mutant cells lacking both Insig-1 and Insig-2, we subjected SRD-14 cells to an additional round of mutagenesis, followed by selection for growth in medium containing a concentration of 25-hydroxycholesterol that blocks the growth of SRD-14 and wild-type cells by accelerating reductase degradation and blocking SREBP processing. Twenty sterol-resistant cell lines were obtained through this procedure; 19 of them were deficient in Insig-2 as well as Insig-1. We studied one of these Insig-1/Insig-2-deficient cells in detail (19).

Previous studies have shown that the regulatory actions of Insigs are critically dependent on the ratios of Insig proteins to their targets (i.e., SCAP and reductase) (4, 12). Overexpression of SCAP or reductase through transfection saturates endogenous Insigs, and regulation no longer occurs unless Insigs are also overexpressed. In the current studies, we characterize the one 25-hydroxycholesterol-resistant CHO cell line, derived from mutagenesis and selection of SRD-14 cells, which continues to produce Insig-2. This cell line, designated SRD-19, was found to have exploited the stoichiometric requirement of Insigs by overproducing SCAP. Indeed, the SCAP gene is amplified and the mRNA is overproduced by 4-fold in SRD-19 cells. These findings support the concept that the ratio of Insigs to its two targets is a crucial requirement for the sterol regulation of cholesterol metabolism.

MATERIALS AND METHODS

Materials

We obtained horseradish peroxidase-conjugated donkey anti-mouse and anti-rabbit IgGs (affinity-purified) from Jackson ImmunoResearch Laboratories; 25-hydroxycholesterol and cholesterol from Steraloids, Inc. (Newport, RI); [^{14}C]acetate and [^{14}C]oleate from American Radiolabeled Chemicals, Inc. (St. Louis, MO); and DECA Template-GAPDH-mouse from Ambion (Austin, TX). SR-12813 was synthesized by the Core Medicinal Chemistry Laboratory, Department of Biochemistry, University of Texas Southwestern Medical Center. Lipoprotein-deficient serum ($d > 1.215$ g/ml) was prepared from newborn calf serum by ultracentrifugation (20). Solutions of sodium compactin and sodium mevalonate were prepared as described previously (21). Other reagents were obtained from sources described previously (22).

Cell culture

All of the cells used in this study were maintained in monolayer culture at 37°C in 8–9% CO_2. CHO-7 cells are a subline of CHO-K1 cells selected for growth in lipoprotein-deficient serum (23). SRD-1, which express constitutively active SREBP-2 resulting from genomic rearrangements of the SREBP-2 gene (24), SRD-14 [deficient in Insig-1 (18)], SRD-15 [deficient in both Insig-1 and Insig-2 (19)], and SRD-19 (overexpresses SCAP resulting from amplification of the SCAP gene; this study) are mutant cell lines derived from CHO-7 cells.

Stock cultures of CHO-7 cells were maintained in medium A (a 1:1 mixture of Ham's F-12 medium and Dulbecco's modified Eagle's medium containing 100 U/ml penicillin and 10 μg/ml streptomycin sulfate) supplemented with 5% (w/v) lipoprotein-deficient serum. SRD-1, SRD-15, and SRD-19 cells were grown in medium A containing 5% lipoprotein-deficient serum and 2.5 μM 25-hydroxycholesterol. SRD-14 cells were maintained in medium A containing 5% lipoprotein-deficient serum and 10 μM SR-12813.

Mutagenesis and isolation of 25-hydroxycholesterol-resistant cells overexpressing SCAP

SRD-19 cells were isolated in the same experiment that yielded Insig-1- and Insig-2-deficient SRD-15 cells (19). Briefly, 2.5×10^7 SRD-14 cells were subjected to γ-irradiation as described previously (18). The mutagenized cells were immediately plated at 5×10^5 cells/100 mm dish in medium A containing 5% lipoprotein-deficient serum. On day 1, cells were refed identical medium containing 1.25 μM 25-hydroxycholesterol. Fresh medium was added to cells every 2 days until colonies formed. On day 29, the surviving colonies were isolated with cloning cylinders and allowed to proliferate. Of the 50 original dishes, 20 contained 25-hydroxycholesterol-resistant colonies; 19 of these colonies exhibited reduced expression of Insig-2, one of which was designated SRD-15 (19). The remaining colony (expressing normal levels of Insig-2) was cloned by limiting dilution and designated SRD-19.

SRD-19 cells stably overexpressing human Insig-1 or Insig-2 were generated as follows. On day 0, SRD-19 cells were set up at 5×10^5 cells per 60 mm dish in medium A containing 5% fetal calf serum, 5 μg/ml cholesterol, 1 mM mevalonate, and 20 μM sodium oleate. On day 1, cells were transfected with 1 μg of pCMV-Insig-1-Myc or pCMV-Insig-2-Myc, expression plasmids encoding human Insig-1 and Insig-2 followed by six tandem copies of the c-Myc epitope (3, 4), using the FuGENE 6 transfection reagent (Roche) as described (25). On day 2, cells were switched to identical medium supplemented with 0.7 mg/ml G418. Fresh medium was added every 2–3 days until colonies formed after ~2 weeks.

Individual colonies were assessed by immunoblot analysis with anti-Myc. Cells from a single colony were cloned by limiting dilution and maintained in medium A containing 5% fetal calf serum, 5 μg/ml cholesterol, 1 mM mevalonate, 20 μM sodium oleate, and 0.5 mg/ml G418 at 37°C, 8–9% CO_2.

Cell fractionation and immunoblot analysis

Triplicate dishes of cells were used to isolate membrane and/or nuclear extract fractions as described previously (12). Aliquots of nuclear extract and membrane fractions were subjected to 8% SDS-PAGE; the proteins were transferred to Hybond C-extra nitrocellulose filters (Millipore) and immunoblot analysis was carried out as described (12). Primary antibodies used for immunoblotting were as follows: IgG-7D4, a mouse monoclonal antibody against the NH_2 terminus of hamster SREBP-2 (26); IgG-2179, a rabbit polyclonal antibody against the NH_2 terminus of hamster SREBP-1c (19); IgG-9E10, a mouse monoclonal antibody against c-Myc purified from the culture medium of hybridoma clone 9E10 (American Type Culture Collection); and IgG-9D5, a mouse monoclonal antibody against hamster SCAP (11).

Neutral lipid staining of cells with Oil Red O

On day 0, CHO-7, SRD-14, SRD-15, and SRD-19 cells were set up for experiments on coverslips as described in the figure legends. On day 3, the cells were fixed with 10% formalin in phosphate-buffered saline for 1 h at room temperature. After washing three times with deionized water, the cells were processed for Oil Red O staining using the dye at a concentration of 4 μg/ml in isopropyl alcohol. Finally, each coverslip was washed for 10 min with deionized water, stained for 5 min with 17 μg/ml 4′,6-diaminophenylindole, and subjected to another 10 min wash with deionized water. Coverslips were then mounted onto glass slides and analyzed on a microscope stage.

Metabolic assays

CHO-7, SRD-14, SRD-15, and SRD-19 cells were set up for experiments as described in the figure legends. The incorporation of [^{14}C]acetate into cellular cholesterol and fatty acids and that of [^{14}C]oleate into cellular cholesteryl esters and triglycerides was measured in cell monolayers as described previously (20, 21). The protein content of cell extracts was determined using the BCA Protein Assay Reagent (Pierce) according to the manufacturer's instructions.

Analysis of lipid droplets isolated from wild-type and mutant CHO cells

On day 0, CHO-7, SRD-14, SRD-15, and SRD-19 cells were set up for experiments as described in the figure legends. On day 1, the cells were labeled with 100 μCi of [^{14}C]acetate for 2 days and collected by scraping in ice-cold PBS containing a protease inhibitor cocktail. Lipid droplet fractions were then purified using a previously described method (27). Total lipids were extracted from purified droplet fractions using a 2:1 (v/v) mixture of acetone and $CHCl_3$, after which an aliquot of the extracted lipids was subjected to scintillation counting. The remaining samples (normalized for equal counts loaded per lane) were separated by thin-layer chromatography on Si gel G60 plates (Whatman) that were developed in a solvent system consisting of 80:20:1 (v/v) hexane-diethyl ether-acetic acid. The migrations of radiolabeled phospholipids, fatty acids, triglycerides, ether lipids, and cholesterols were determined by visualizing unlabeled standards with iodine vapor. The region corresponding to the various lipids was collected by scraping and subjected to scintillation counting.

Determination of cellular sterol composition

CHO-7, SRD-14, SRD-15, and SRD-19 cells were set up for experiments on day 0 as described in the figure legends. On day 3, cell monolayers were washed with buffer containing 5 mM Tris-HCl (pH 7.4), 150 mM NaCl, and 0.2% BSA, followed by an additional wash in an identical buffer containing no BSA. Subsequently, 1 ml of wash buffer containing no BSA was added to each dish; the cells were harvested by scraping, transferred to a 1.5 ml Eppendorf tube, and subjected to centrifugation for 5 min at 4,000 rpm at 4°C. After removal of the supernatant, the cell pellets were resuspended in 1 ml of 0.1 M NaOH and vortexed at room temperature for 30 min. An aliquot of the resulting cell lysates was used to determine protein concentration as described above. An ethanolic solution containing the internal standards 5α-cholestane (50 μg) and epicoprostanol (2.5 μg) was added to 200 μl of the remaining cell lysates, and sterols were hydrolyzed by heating (to 100°C) in ethanolic KOH (100 mM) for 2 h. Lipids were extracted in petroleum ether, dried under nitrogen, and derivatized with hexamethyldisilazane-trimethylchlorosilane. GC-MS analysis was performed using a 6890N gas chromatograph coupled to a 5973 mass selective detector (Agilent Technologies, Palo Alto, CA). Trimethylsilyl-derived sterols were separated on an HP-5MS 5%-phenyl methyl polysiloxane capillary column (30 m × 0.25 mm inside diameter × 0.25 μm film) with carrier gas helium at the rate of 1 ml/min. The temperature program was 150°C for 2 min, followed by increasing the temperature by 20°C per minute up to 280°C and holding it for 13 min. The injector was operated in the splitless mode and was kept at 280°C. The mass spectrometer was operated in selective ion monitoring mode. The extracted ions were 458.4 (cholesterol), 343.3 (desmosterol), 458.4 (lathosterol), 441.4 (zymosterol), 393.4 (lanosterol), and 350.4 (7-dehydrocholesterol).

Real-time PCR and Northern and Southern blot analyses

The protocol for real-time PCR was identical to that described by Liang et al. (28). Total RNA was isolated from CHO-7, SRD-13A, SRD-14, SRD-15, and SRD-19 cells using the RNeasy kit (Qiagen) according to the manufacturer's instructions and subjected to reverse transcription reactions. Triplicate samples of reverse-transcribed total RNA were subjected to real-time PCR quantification using forward and reverse primers for hamster Insig-1, Insig-2, SCAP, FAS, stearoyl-CoA desaturase-1, LDL receptor, HMG-CoA synthase, and HMG-CoA reductase. Relative amounts of mRNAs were calculated using the comparative threshold cycle method. Hamster SREBP-2 cDNA probe was prepared by PCR amplification using the following primers: 5′-ATGGACGAGAG-CAGCGAGCTGGGCGG-3′ and 5′-ACAGGAGGAGAGTCTGGTT-CATC-3′. Hamster SCAP was also generated by PCR as described previously. The resulting PCR products and the mouse GAPDH probe were radiolabeled with [α-^{32}P]dCTP using the Megaprime DNA Labeling System (Amersham Biosciences). Total RNA and restriction enzyme-digested genomic DNA were subjected to electrophoresis and transferred to Hybond N^+ membranes (Amersham Biosciences), and the filters were hybridized at 60–68°C with radiolabeled probes (2×10^6 cpm/ml and 4×10^6 cpm/ml for Northern and Southern blots, respectively) using the ExpressHyb Hybridization Solution (Clontech) according to the manufacturer's instructions. Filters were exposed to film with intensifying screens for the indicated times at −80°C.

RESULTS

Table 1 lists the cell lines used in this study. SRD-14 cells (for sterol-regulatory defective) are Insig-1-deficient cells

TABLE 1. Cell lines used

Cell Line	Description	Source
CHO-K1	Parental cells for all lines used in this study	American Type Culture Collection No. CRL-9618
CHO-7	Subline of CHO-K1 cells selected for growth in lipoprotein-deficient serum	Ref. 23
SRD-1	Mutant CHO-7 cells that express constitutively active SREBP-2 resulting from genomic rearrangements of the *SREBP-2* gene	Ref. 24
SRD-14	Mutant CHO-7 cells lacking Insig-1	Ref. 18
SRD-15	Mutant CHO-7 cells lacking Insig-1 and Insig-2	Ref. 19
SRD-19	Mutant CHO-7 cells lacking Insig-1 and harboring the amplified sterol-regulatory element binding protein cleavage-activating protein gene	This study

CHO, Chinese hamster ovary; SREBP, sterol-regulatory element binding protein.

derived from CHO-7 cells by mutagenesis with γ-irradiation and selection with SR-12813 (18). SRD-15 and SRD-19 cells were derived from SRD-14 cells by mutagenesis with γ-irradiation and selection with 1.25 μM 25-hydroxycholesterol as described in Ref. 19 and in Materials and Methods. SRD-15 cells are deficient in Insig-2 as well as Insig-1 and, as a result, neither stimulate the ubiquitination/degradation of reductase nor suppress the processing of SREBPs in response to treatment with 25-hydroxycholesterol. SRD-19 cells were not characterized previously. In unpublished studies, we found that SRD-19 cells survived culture in medium that contained up to 2.5 μM 25-hydroxycholesterol; similar results were obtained with SRD-15 cells and SRD-1 cells (which express truncated, constitutively active SREBP-2).

We compared lipid synthesis in wild-type and mutant cells by growing the cells in the absence of exogenous cholesterol and then metabolically labeling them with [^{14}C]acetate for 2 h, after which incorporation of the radiolabel into cholesterol and fatty acids was measured. **Table 2** shows that when grown in lipoprotein-deficient serum, SRD-14 cells incorporated ~2.5-fold more [^{14}C]acetate into cholesterol than wild-type CHO-7 cells; the rate of [^{14}C]cholesterol synthesis was even higher in SRD-15 and SRD-19 cells (4.8- and 6.8-fold, respectively). In a similar manner, [^{14}C]acetate labeling of fatty acids was increased in SRD-14 (1.3-fold), SRD-15 (3.4-fold), and SRD-19 (4.6-fold) cells relative to that in CHO-7 cells.

TABLE 2. Incorporation of [^{14}C]acetate into [^{14}C]cholesterol and ^{14}C-labeled fatty acids in parental CHO-7 cells and mutant cells resistant to 25-hydroxycholesterol

Cell Line	Incorporation of [^{14}C]Acetate	
	[^{14}C]Cholesterol	^{14}C-Labeled Fatty Acids
	nmol/h/mg protein	
CHO-7	0.159 ± 0.011	0.278 ± 0.023
SRD-14	0.396 ± 0.012	0.375 ± 0.127
SRD-15	0.777 ± 0.019	0.937 ± 0.017
SRD-19	1.076 ± 0.070	1.271 ± 0.027

On day 0, monolayers of cells were set up for experiments at 1×10^5 cells per 60 mm dish in medium A supplemented with 5% lipoprotein-deficient serum. On day 2, the cells were refed the identical medium containing 10 μCi/dish [^{14}C]acetate. After incubation at 37°C for 2 h, the cells were harvested for measurement of the cellular content of [^{14}C]cholesterol and ^{14}C-labeled fatty acids. A blank value, representing the amount of [^{14}C]acetate incorporated into [^{14}C]cholesterol (0.15 nmol/h/mg) and ^{14}C-labeled fatty acids (0.03 nmol/h/mg) in each cell line that was incubated for 2 h at 4°C, was subtracted from each value. Each value is the mean of triplicate incubations.

The results in Table 2 led us to next compare the sterol composition of wild-type CHO-7 and mutant SRD cells. The cells were cultured for 3 days in lipoprotein-deficient serum, after which they were harvested and lysed. Lipids were extracted from the resulting cell lysates and analyzed by gas chromatography-mass spectroscopy, which revealed total sterol levels of 38, 70, 117, and 110 μg/mg protein for CHO-7, SRD-14, SRD-15, and SRD-19 cells, respectively (**Fig. 1A**). As expected, cholesterol was the most abundant sterol in each cell line (>70% of total sterol content), and levels of the sterol were increased by 2- to 4-fold in the mutant cells (Fig. 1B). The cholesterol synthesis intermediate 7-dehydrocholesterol was increased in SRD-15 and SRD-19 cells, whereas lathosterol and zymosterol levels remained unchanged. Lanosterol, the first sterol produced in cholesterol synthesis, was increased dramatically in SRD-15 cells (>10-fold) and to a lesser extent (~5-fold) in SRD-19 cells. The level of desmosterol was also increased in SRD-15 cells, but not to the same magnitude as lanosterol. Similar results were obtained in at least two other independent experiments.

Lipid droplets, also termed lipid particles or lipid bodies (29), are generally regarded as storage depots for neutral lipids, such as triglycerides and cholesteryl esters. To determine whether the increase in cholesterol synthesis and total sterol content of SRD-14, SRD-15, and SRD-19 cells correlated with an increase in lipid droplet formation, cells were stained with the lipid-specific dye Oil Red O. **Figure 2A** shows that CHO-7 cells accumulated lipid droplets of varying size after 3 days of culture in lipoprotein-deficient serum. The number and size of lipid droplets increased markedly in SRD-14, SRD-15, and SRD-19 cells.

We next conducted a compositional analysis of lipid droplet fractions isolated from wild-type and mutant cells. The cells were metabolically labeled for 2 days with [^{14}C]acetate and harvested, and the lipid droplet fractions were isolated using a standard procedure developed previously (27). Equal amounts of ^{14}C-labeled lipids extracted from the resulting fractions were then subjected to thin-layer chromatography, and incorporation of radiolabel into various lipids was determined by scintillation counting. Figure 2B shows that >50% of [^{14}C]acetate was incorporated into cholesteryl esters in CHO-7 cells; ~30% of the radiolabel appeared in triglycerides. The percentage of [^{14}C]acetate incorporation into cholesteryl esters was

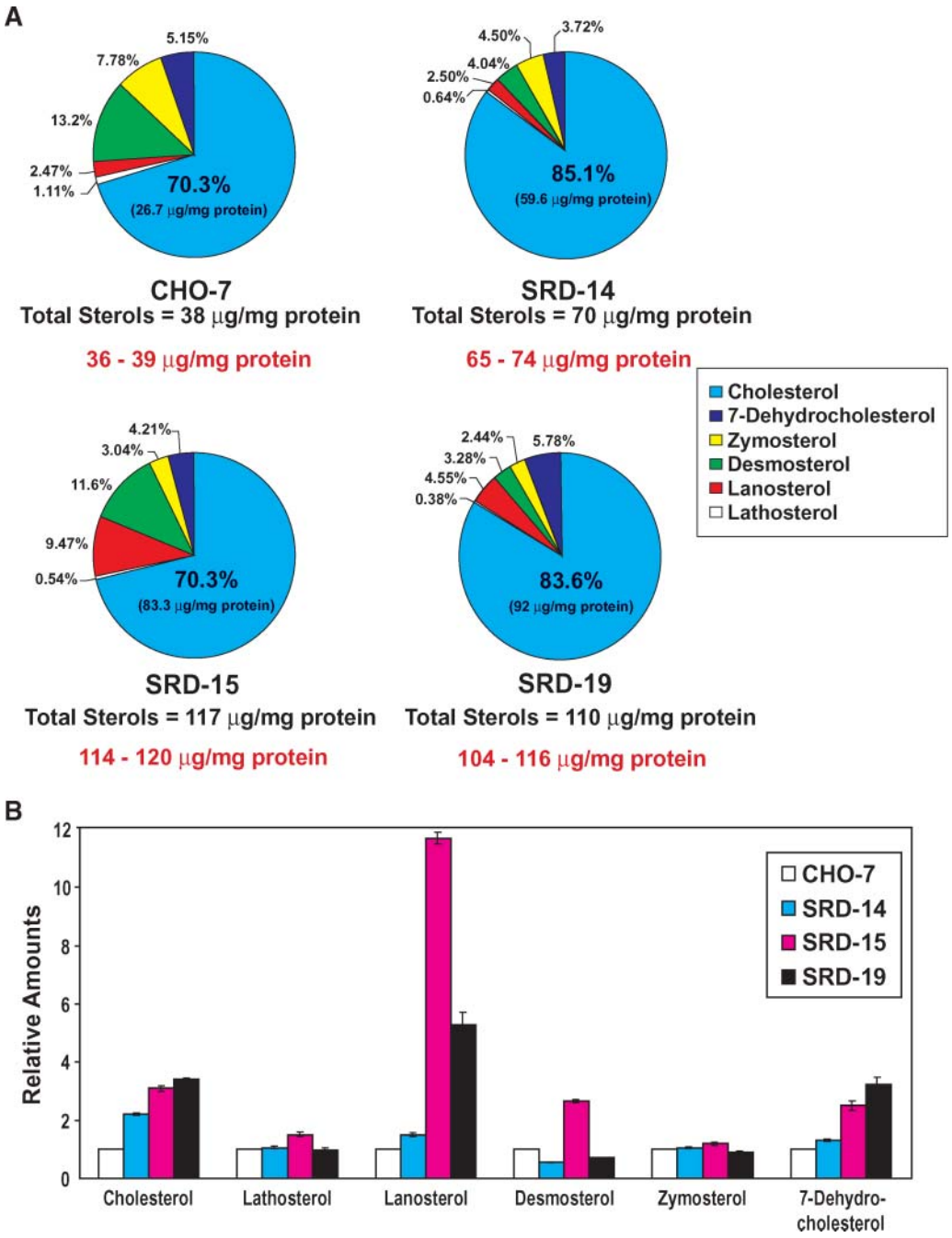

Fig. 1. Sterol content of wild-type Chinese hamster ovary (CHO)-7 and mutant SRD-14, SRD-15, and SRD-19 cells. CHO-7, SRD-14, SRD-15, and SRD-19 cells were set up on day 0 at 5×10^5 cells per 100 mm dish in medium A supplemented with 5% lipoprotein-deficient serum. On day 3, the cells were harvested, lysed, and subjected to GC-MS analysis as described in Materials and Methods. In A, each sterol is reported as a percentage of total sterols in the various cell lines. The ranges in amounts of total sterols obtained for three independent experiments are indicated in red. In B, the values for each sterol are reported relative to those in parental CHO-7 cells, which are arbitrarily set at 1. Error bars indicate ± SEM.

increased by ~14, 29, and 11% in SRD-14, SRD-15, and SRD-19 cells, respectively. Conversely, incorporation of radiolabel into triglycerides was reduced by 5–20% in the mutant cell lines. Similar results were obtained in an independent experiment.

For **Fig. 3**, we labeled CHO-7, SRD-14, SRD-15, and SRD-19 cells with [^{14}C]oleate and subsequently measured the formation of cholesteryl [^{14}C]oleate and ^{14}C-labeled triglycerides in the presence of varying concentrations of LDL or 25-hydroxycholesterol. SRD-15 and SRD-19 cells exhibited a slightly increased level of basal cholesteryl [^{14}C]oleate formation, which likely results from the increased levels of cholesterol synthesis in the cells (Table 2). In all of the cell lines, LDL and 25-hydroxycholesterol

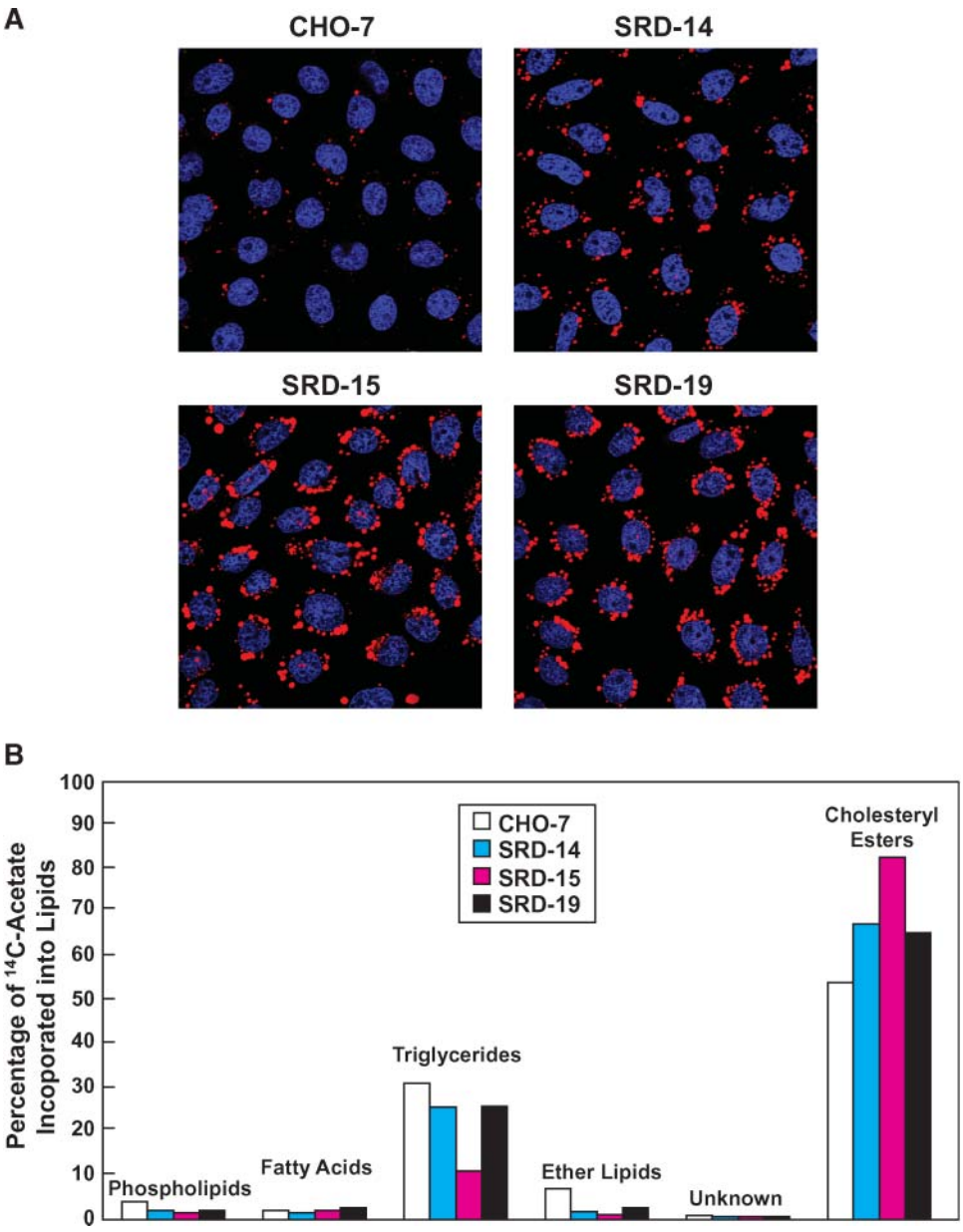

Fig. 2. Accumulation of neutral lipids in CHO-7, SRD-14, SRD-15, and SRD-19 cells as revealed by Oil Red O staining. A: On day 0, CHO-7, SRD-14, SRD-15, and SRD-19 cells were set up at 1×10^5 cells per 37 mm dish with coverslips in medium A supplemented with 5% lipoprotein-deficient serum. On day 3, the cells were fixed and double stained with 4′,6-diamino-phenylindole for nuclei (blue) and with Oil Red O for lipid droplets (red) as described in Materials and Methods. B: On day 0, CHO-7, SRD-14, SRD-15, and SRD-19 cells were set up at 5×10^5 cells per 100 mm dish in medium A containing 5% fetal calf serum. On day 1, the cells were refed the identical medium containing 100 μCi of [^{14}C]acetate and incubated for an additional 2 days at 37°C. The cells were subsequently harvested and lysed, and lipid droplet fractions were isolated and analyzed by thin-layer chromatography. The percentage of [^{14}C]acetate incorporated into the indicated lipids was determined by scintillation counting.

stimulated the incorporation of [^{14}C]oleate into cholesteryl [^{14}C]oleate in a dose-dependent manner. LDL and 25-hydroxycholesterol did not stimulate the incorporation of [^{14}C]oleate into ^{14}C-labeled triglycerides in any of the cell lines.

The resistance of SRD-19 cells to 25-hydroxycholesterol-induced death, coupled with increased cholesterol synthesis and overaccumulation of sterols (Table 2, Fig. 1), indicates a disruption in the feedback mechanism that controls the production of cholesterol. Thus, we next compared the sterol regulation of SREBP processing in CHO-7, SRD-14, SRD-15, SRD-19, and SRD-1 cells. In the experiment shown in **Fig. 4**, the cells were incubated in medium containing lipoprotein-deficient serum, the reductase inhibitor compactin, and 50 μM mevalonate to ensure cell viability. Some of the dishes also received 1.25 μM

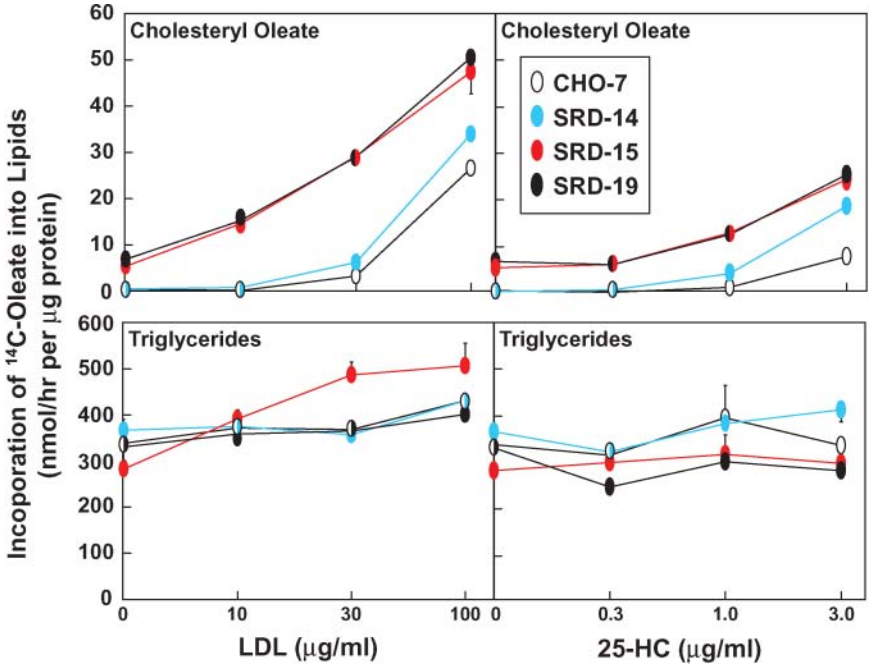

Fig. 3. Effects of LDL and 25-hydroxycholesterol (25-HC) on the incorporation of [^{14}C]oleate into cholesteryl [^{14}C]oleate and ^{14}C-labeled triglycerides in wild-type and mutant CHO cells. On day 0, cells were set up at 1×10^5 cells per 60 mm dish in medium A containing 5% lipoprotein-deficient serum. On day 2, the cells were switched to medium A containing 5% lipoprotein-deficient serum, 50 μM sodium compactin, and 50 μM sodium mevalonate. On day 2, the cells were refed the identical medium with either no addition or the indicated concentrations of LDL or 25-hydroxycholesterol. After incubation for 5 h at 37°C, cells were pulsed for 2 h with 0.2 mM [^{14}C]oleate/albumin (10 dpm/nmol), after which the cells were harvested for measurement of their content of cholesteryl [^{14}C]oleate and [^{14}C]triglycerides. Each value is the mean of triplicate incubations. Error bars indicate ± SEM.

25-hydroxycholesterol. After 16 h, the cells were harvested and separated into membrane and nuclear extract fractions. Immunoblot analysis of the fractions was subsequently carried out with antibodies against SREBP-1 (Fig. 4, top panel), SREBP-2 (middle panel), and SCAP (bottom panel). Bands corresponding to processed forms of SREBP-1 and SREBP-2 were observed in nuclear extracts from untreated CHO-7, SRD-14, SRD-15, and SRD-19 cells (top and middle panels, lanes 1, 3, 5, 7). In CHO-7 and SRD-14 cells, 25-hydroxycholesterol inhibited the processing of both SREBPs after the 16 h incubation (lanes 2, 4), whereas SREBP processing in SRD-15 and SRD-19 cells continued (lanes 6, 8). A 25-hydroxycholesterol-resistant, truncated form of nuclear SREBP-2 was observed in the absence of nuclear SREBP-1 for SRD-1 cells (lanes 9, 10). The absence of nuclear SREBP-1 in SRD-1 cells is attributable to the constitutively active SREBP-2 that stimulates the overproduction of cholesterol, which in turn prevents SCAP-mediated processing of the membrane-bound SREBP-1 precursor (24).

The membrane fractions from CHO-7, SRD-14, SRD-15, and SRD-1 cells contained similar amounts of SCAP that were not affected by the absence or presence of 25-hydroxycholesterol (Fig. 4, bottom panel, lanes 1–6, 9, 10). However, a marked increase in SCAP protein was observed in SRD-19 cells (lanes 7, 8). These results led us to conduct a set of experiments to determine the molecular defect that leads to the overproduction of SCAP protein in SRD-19 membranes. The quantitative real-time PCR experiment shown in **Fig. 5A** revealed that SRD-19 cells express >4.5-fold more SCAP mRNA than their wild-type CHO-7 counterparts and ~3-fold more than parental SRD-14 cells. The level of SCAP mRNA was not influenced by the presence of 25-hydroxycholesterol. As expected, SREBP target genes, including Insig-1, FAS, stearoyl-CoA desaturase-1, LDL receptor, and HMG-CoA synthase and reductase, were downregulated in wild-type and SRD-14 cells treated with 25-hydroxycholesterol. In contrast, these genes were refractory to sterol regulation in SRD-15 and SRD-19 cells. Notably, stearoyl-CoA desaturase-1 mRNA was more induced in SRD-15 cells, for reasons that are not clear.

In the experiment shown in Fig. 5B, restriction enzyme-digested genomic DNA from CHO-7 and SRD-19 cells was subjected to agarose gel electrophoresis, transferred to nylon membranes, and hybridized with radiolabeled SCAP (top panel) or SREBP-2 (bottom panel) cDNA probes. Each restriction enzyme digest of CHO-7 and SRD-19 genomic DNA produced fragments of identical size that hybridized with the SCAP and SREBP-2 probes, but the intensities of SCAP-hybridizing fragments were markedly increased in the SRD-19 digests (top and bottom panels, lanes 1–16). The intensities of fragments that hybridized to the SREBP-2 probe were similar in enzyme-digested genomic DNA from CHO-7 and SRD-19 cells (bottom panel). In Fig. 5C, various amounts of enzyme-digested DNA from

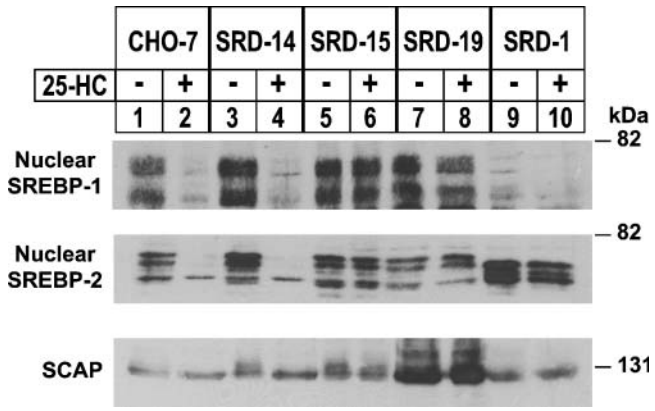

Fig. 4. Sterol regulation of sterol-regulatory element binding protein (SREBP) processing in wild-type and mutant CHO cells. On day 0, CHO-7, SRD-14, SRD-15, SRD-19, and SRD-1 cells were set up at 5×10^5 cells per 100 mm dish in medium A supplemented with 5% lipoprotein-deficient serum. On day 2, the cells were switched to medium A containing 5% lipoprotein-deficient serum, 10 μM compactin, and 50 μM mevalonate in the absence (−) or presence (+) of 2.5 μM 25-hydroxycholesterol (25-HC). After incubation for 16 h at 37°C, cells were harvested and subjected to cell fractionation. Aliquots of membrane (27 μg protein/lane) and nuclear extract (15 μg protein/lane) fractions were subjected to SDS-PAGE and transferred to nylon membranes. Immunoblot analysis was carried out with 5 μg/ml IgG-7D4 (against SREBP-2), 5 μg/ml IgG-2179 (against SREBP-1), and 5 μg/ml IgG-9D5 [against sterol-regulatory element binding protein cleavage-activating protein (SCAP)]. Filters were exposed to film at room temperature for 20 s to 3 min.

CHO-7 and SRD-19 cells were hybridized with radiolabeled SCAP and SREBP-2 cDNA probes. By densitometric scanning, we calculated an ~4- to 5-fold increase in the amount of hybridizable SCAP DNA in SRD-19 cells compared with CHO-7 cells. These results indicate that the SCAP gene is amplified in SRD-19 cells, which likely accounts for the overproduction of SCAP mRNA and protein in the mutant cells.

When transfected cells overexpress SCAP, the Insig proteins become saturated and 25-hydroxycholesterol can no longer inhibit SREBP processing. Oxysterol-mediated inhibition can be restored by coexpression of either Insig-1 (4) or Insig-2 (3). If overproduction of SCAP is the primary defect in SRD-19 cells, the regulatory effects of 25-hydroxycholesterol should be restored by overexpressing Insig-1 or Insig-2. Thus, SRD-19 cells were transfected with pCMV-Insig-1-Myc or pCMV-Insig-2-Myc, expression plasmids encoding human Insig-1 and Insig-2, respectively, followed by six tandem copies of the c-Myc epitope. Clones that expressed equivalent levels of the Myc-tagged Insig proteins were isolated (**Fig. 6**, bottom panel) and analyzed further. As expected, SREBP-2 processing was sensitive to 25-hydroxycholesterol in wild-type CHO-7 cells (top panel, lanes 1, 2) and resistant to sterol treatment in mock-transfected SRD-19 cells (lanes 3, 4). Overexpression of Insig-1-Myc or Insig-2-Myc in SRD-19 cells restored a complete response to 25-hydroxycholesterol (lanes 5–8). Overexpression of either Insig in SRD-19 cells also restored the 25-hydroxycholesterol-mediated suppression of SREBP-1 processing (data not shown).

DISCUSSION

The current data describe the characterization of SRD-19 cells, a line of mutant CHO cells that were produced by mutagenesis of Insig-1-deficient SRD-14 cells (19), followed by selection for growth in 25-hydroxycholesterol. Because of their resistance to 25-hydroxycholesterol, SRD-19 cells fail to suppress the proteolytic activation of SREBPs upon prolonged treatment with the sterol (Fig. 4). This resistance is accompanied by the amplification of the gene encoding SCAP (Fig. 5B, C), which leads to the overproduction of SCAP mRNA and protein (Figs. 4, 5). Although the number of copies of the SCAP gene is apparently increased in SRD-19 cells, the gene does not appear to have undergone any gross structural rearrangements, at least at the level that is detectable by the cDNA probe used here.

A reasonable explanation for the resistance of SRD-19 cells to 25-hydroxycholesterol is that excess SCAP saturates the remaining Insig-2 in the mutant cells. As a result, SREBPs continue to be processed and cholesterol synthesis is not inhibited, even in the presence of 25-hydroxycholesterol. Accordingly, SRD-19 cells are resistant to chronic culture in the oxysterol. Evidence in support of this conclusion is provided by the experiment shown in Fig. 6, which shows that overexpression of cDNAs encoding either Insig-1 or Insig-2 restores normal sterol regulation of SREBP processing in SRD-19 cells. Our finding that SCAP overproduction causes resistance of SRD-19 cells to culture in 25-hydroxycholesterol is analogous to the resistance of UT-1 cells to growth in the HMG-CoA reductase inhibitor compactin. UT-1 cells, a line of mutant CHO cells isolated in 1982 (30), grow in the presence of compactin owing to the >100-fold overproduction of reductase, which results from the amplification and enhanced transcription of the gene encoding the enzyme (31).

Consistent with the partial (SRD-14) and complete (SRD-15 and SRD-19) resistance to 25-hydroxycholesterol, rates of cholesterol and fatty acid synthesis were increased markedly in the mutant cells (Table 2). Moreover, accumulations of total sterol (Fig. 1) and neutral lipid content (as determined by Oil Red O staining; Fig. 2) were observed in SRD-14, SRD-15, and SRD-19 cells in proportion to their resistance to 25-hydroxycholesterol (Fig. 4). Cholesterol was the most abundant sterol in CHO-7, SRD-14, SRD-15, and SRD-19 cells, and its levels were increased by 2- to 4-fold in mutant cells compared with wild-type cells (Fig. 1). Several intermediates in the cholesterol biosynthetic pathway were only increased in SRD-15 and SRD-19 cells. Specifically, lanosterol, the first sterol intermediate in cholesterol synthesis, was increased by 11-fold in SRD-15 cells and by 5-fold in SRD-19 cells. This is an interesting finding with regard to results from a previous study, which suggested that the production of lanosterol is a key focal point of the sterol regulatory system (32). In normal cells, lanosterol triggers the ubiquitination and rapid degrada-

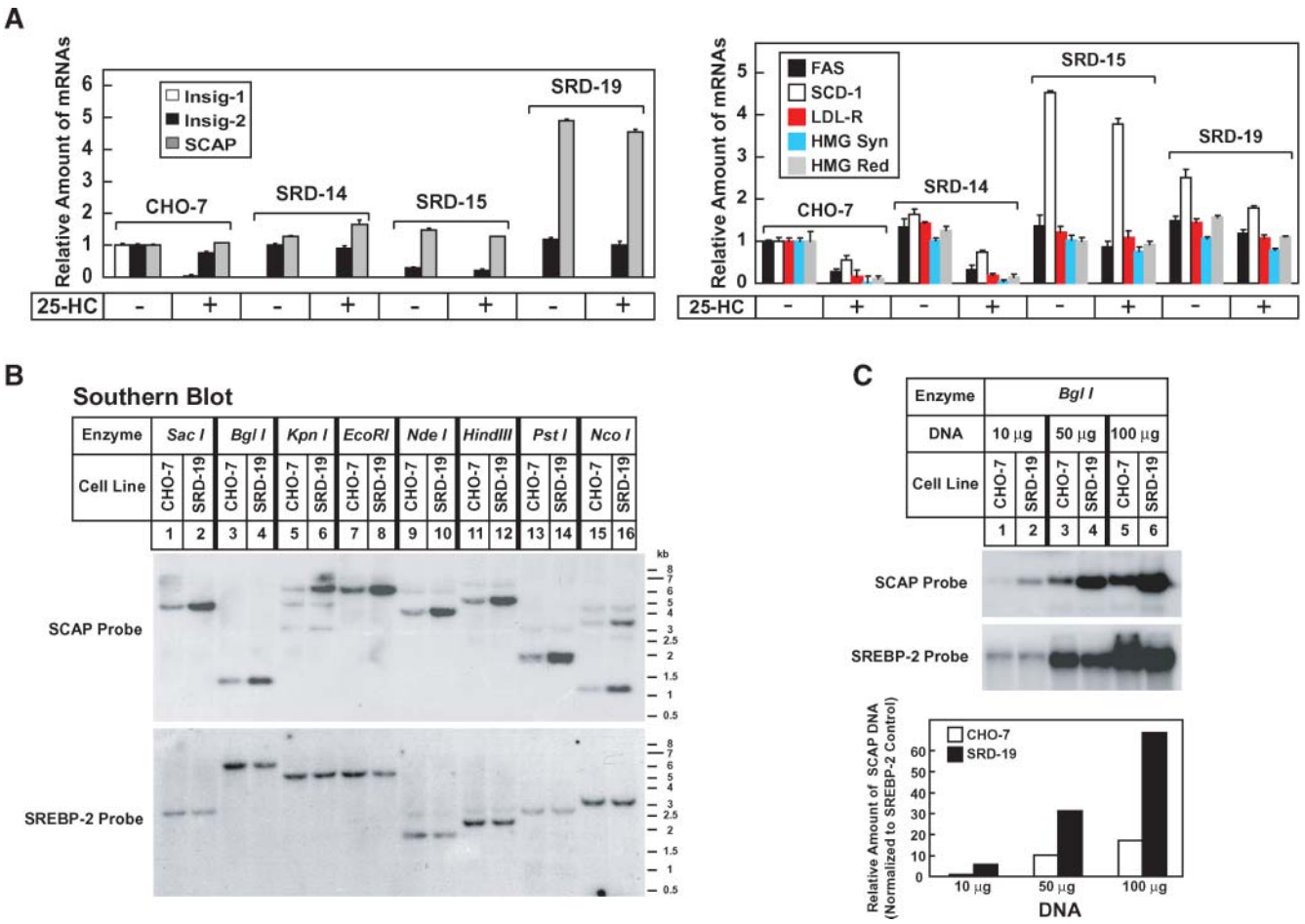

Fig. 5. Molecular characterization of SCAP mRNA and genomic DNA in parental CHO-7 and mutant SRD-19 cells. A: CHO-7, SRD-14, SRD-15, and SRD-19 cells were set up on day 0 and treated on day 2 as described in the legend to Fig. 4. After incubation for 16 h at 37°C in the absence (−) or presence (+) of 25-hydroxycholesterol (25-HC), cells were harvested for isolation of total RNA, which was subjected to quantitative real-time PCR analysis using specific primers for the indicated genes. The relative amount of mRNA under each condition was normalized to an internal control gene (GAPDH). SCD-1, stearoyl-coenzyme A desaturase-1. B, C: Aliquots of genomic DNA (20 µg/lane in B; the indicated amounts in C) from CHO-7 and SRD-19 cells were digested with the indicated restriction enzymes, subjected to electrophoresis, and transferred to nylon filters. Hybridizations were carried out with ^{32}P-labeled cDNA probes corresponding to SCAP (nucleotides 1–697) or SREBP-2 (nucleotides 1–460). The filters were exposed to film at −80°C for 24 h (SCAP) and 48 h (SREBP-2). In C, filters were also exposed to an imaging plate for 12 h at room temperature and scanned in a Storm 820 phosphorimager, and the amounts of hybridized SCAP and SREBP probes were quantified. Error bars indicate ± SEM.

tion of HMG-CoA reductase, thereby reducing carbon flow through the cholesterol synthetic pathway. Inappropriate accumulation of lanosterol is prevented by its inability to block SREBP processing by inhibiting the activity of SCAP. Thus, mRNAs encoding enzymes that catalyze reactions subsequent to lanosterol remain increased, and lanosterol is metabolized to cholesterol. The accumulation of cholesterol triggers the ER retention of SCAP-SREBP complexes, which leads to the inhibition of SREBP processing and ultimately shuts down the entire cholesterol synthetic pathway. In SRD-15 and SRD-19 cells, this feedback regulation is lost, and as a result, cholesterol and its sterol precursors accumulate inappropriately. It should be noted that C-14 demethylation, the initial step in the conversion of lanosterol to cholesterol, has been implicated as a rate-limiting step in cholesterol synthesis (33, 34). This might help to explain the selective increase in the level of lanosterol in SRD-15 and SRD-19 cells. Alternatively, Insigs (whose activities are reduced in SRD-15 and SRD-19 cells) may directly or indirectly participate in the demethylation of lanosterol. Future studies will be aimed at resolving these issues.

Three types of mutant CHO cells have been classified as resistant to 25-hydroxycholesterol owing to their failure to suppress cholesterol synthesis under conditions of sterol overload (19, 35). Type 1 mutants express truncated forms of SREBP-2 that migrate to the nucleus and activate gene transcription regardless of sterol treatment. Type 2 mutants express forms of SCAP that harbor point mutations in the sterol-sensing domain that prevents binding to Insigs. These mutant forms of SCAP continue to transport SREBPs to the Golgi even when cells are overloaded with sterols. Type 3 mutants have deficiencies in Insig-1 and Insig-2, and as a result, both reductase and SCAP are refrac-

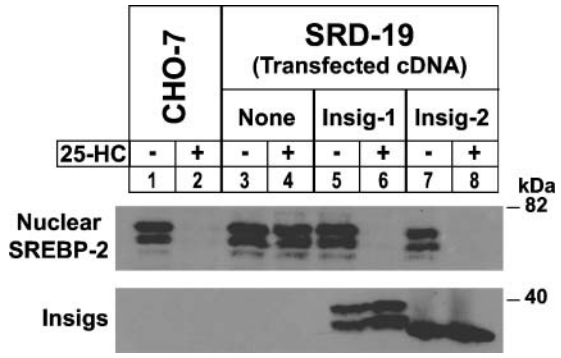

Fig. 6. Stable transfection of pCMV-Insig-1-Myc or pCMV-Insig-2-Myc restores sterol-mediated suppression of SREBP-2 processing in SRD-19 cells. Cells were set up on day 0 and treated on day 2 as described in the legend to Fig. 4. After incubation for 16 h at 37°C in the absence (−) or presence (+) of 25-hydroxycholesterol (25-HC), cells were harvested and membrane and nuclear extract fractions were prepared and subjected to immunoblot analysis with 5 μg/ml IgG-7D4 (against SREBP-2) and 5 μg/ml IgG-9E10 (against Insig-1-Myc or Insig-2-Myc). Filters were exposed to film at room temperature for 3 s to 1 min.

tory to sterol regulation. Data from the current study demonstrate that SRD-19 cells represent a fourth type of 25-hydroxycholesterol-resistant cells. SRD-19 cells have exploited the stoichiometric relationship between Insigs and their targets (reductase and SCAP) by overproducing SCAP. The overexpressed SCAP saturates the remaining Insig-2 in SRD-19 cells, rendering them refractory to sterol regulation. Considering *1*) that the other 19 cell lines isolated in the same mutagenesis/selection experiment that yielded SRD-19 cells were deficient in Insig-1 and Insig-2 and *2*) the unbiased selection for 25-hydroxycholesterol resistance in these experiments, it is likely that the spectrum of proteins participating in the Insig-mediated regulation of sterol metabolism is known and that our knowledge of the mechanism underlying the process is near completion.

The authors thank Drs. Michael S. Brown and Joseph L. Goldstein for their continued encouragement and advice and their evaluation of the manuscript. The authors also thank Jonathan C. Cohen and Fang Xu for help in determining the sterol composition of wild-type and mutant SRD cells, Tammy Dinh and Kristi Garland for excellent technical assistance, and Lisa Beatty for help with tissue culture. This work was supported by grants from the National Institutes of Health (Grant HL-20948) and the Perot Family Foundation. R.A.D-B. is the recipient of a National Institutes of Health Mentored Minority Faculty Development Award (Grant HL-70441), an Established Investigator Award from the American Heart Association (Grant 0540128N), and a Distinguished Young Investigator in Medical Research Award from the W. M. Keck Foundation.

REFERENCES

1. Horton, J. D., N. A. Shah, J. A. Warrington, N. N. Anderson, S. W. Park, M. S. Brown, and J. L. Goldstein. 2003. Combined analysis of oligonucleotide microarray data from transgenic and knockout mice identifies direct SREBP target genes. *Proc. Natl. Acad. Sci. USA.* **100:** 12027–12032.
2. Radhakrishnan, A., L. P. Sun, H. J. Kwon, M. S. Brown, and J. L. Goldstein. 2004. Direct binding of cholesterol to the purified membrane region of SCAP: mechanism for a sterol-sensing domain. *Mol. Cell.* **15:** 259–268.
3. Yabe, D., M. S. Brown, and J. L. Goldstein. 2002. Insig-2, a second endoplasmic reticulum protein that binds SCAP and blocks export of sterol regulatory element-binding proteins. *Proc. Natl. Acad. Sci. USA.* **99:** 12753–12758.
4. Yang, T., P. J. Espenshade, M. E. Wright, D. Yabe, Y. Gong, R. Aebersold, J. L. Goldstein, and M. S. Brown. 2002. Crucial step in cholesterol homeostasis: sterols promote binding of SCAP to INSIG-1, a membrane protein that facilitates retention of SREBPs in ER. *Cell.* **110:** 489–500.
5. Goldstein, J. L., and M. S. Brown. 1990. Regulation of the mevalonate pathway. *Nature.* **343:** 425–430.
6. Song, B. L., N. Sever, and R. A. DeBose-Boyd. 2005. Gp78, a membrane-anchored ubiquitin ligase, associates with Insig-1 and couples sterol-regulated ubiquitination to degradation of HMG CoA reductase. *Mol. Cell.* **19:** 829–840.
7. Liscum, L., J. Finer-Moore, R. M. Stroud, K. L. Luskey, M. S. Brown, and J. L. Goldstein. 1985. Domain structure of 3-hydroxy-3-methylglutaryl coenzyme A reductase, a glycoprotein of the endoplasmic reticulum. *J. Biol. Chem.* **260:** 522–530.
8. Nohturfft, A., M. S. Brown, and J. L. Goldstein. 1998. Topology of SREBP cleavage-activating protein, a polytopic membrane protein with a sterol-sensing domain. *J. Biol. Chem.* **273:** 17243–17250.
9. Roitelman, J., E. H. Olender, S. Bar-Nun, W. A. Dunn, Jr., and R. D. Simoni. 1992. Immunological evidence for eight spans in the membrane domain of 3-hydroxy-3-methylglutaryl coenzyme A reductase: implications for enzyme degradation in the endoplasmic reticulum. *J. Cell Biol.* **117:** 959–973.
10. Gil, G., J. R. Faust, D. J. Chin, J. L. Goldstein, and M. S. Brown. 1985. Membrane-bound domain of HMG CoA reductase is required for sterol-enhanced degradation of the enzyme. *Cell.* **41:** 249–258.
11. Sakai, J., A. Nohturfft, D. Cheng, Y. K. Ho, M. S. Brown, and J. L. Goldstein. 1997. Identification of complexes between the COOH-terminal domains of sterol regulatory element-binding proteins (SREBPs) and SREBP cleavage-activating protein. *J. Biol. Chem.* **272:** 20213–20221.
12. Sever, N., T. Yang, M. S. Brown, J. L. Goldstein, and R. A. DeBose-Boyd. 2003. Accelerated degradation of HMG CoA reductase mediated by binding of insig-1 to its sterol-sensing domain. *Mol. Cell.* **11:** 25–33.
13. Brown, M. S., and J. L. Goldstein. 1999. A proteolytic pathway that controls the cholesterol content of membranes, cells, and blood. *Proc. Natl. Acad. Sci. USA.* **96:** 11041–11048.
14. Kuwabara, P. E., and M. Labouesse. 2002. The sterol-sensing domain: multiple families, a unique role? *Trends Genet.* **18:** 193–201.
15. Hua, X., A. Nohturfft, J. L. Goldstein, and M. S. Brown. 1996. Sterol resistance in CHO cells traced to point mutation in SREBP cleavage-activating protein. *Cell.* **87:** 415–426.
16. Lee, P. C., A. D. Nguyen, and R. A. DeBose-Boyd. 2007. Mutations within the membrane domain of HMG-CoA reductase confer resistance to sterol-accelerated degradation. *J. Lipid Res.* **48:** 318–327.
17. Sever, N., B. L. Song, D. Yabe, J. L. Goldstein, M. S. Brown, and R. A. DeBose-Boyd. 2003. Insig-dependent ubiquitination and degradation of mammalian 3-hydroxy-3-methylglutaryl-CoA reductase stimulated by sterols and geranylgeraniol. *J. Biol. Chem.* **278:** 52479–52490.
18. Sever, N., P. C. W. Lee, B. L. Song, R. B. Rawson, and R. A. DeBose-Boyd. 2004. Isolation of mutant cells lacking Insig-1 through selection with SR-12813, an agent that stimulates degradation of 3-hydroxy-3-methylglutaryl-coenzyme A reductase. *J. Biol. Chem.* **279:** 43136–43147.
19. Lee, P. C., N. Sever, and R. A. DeBose-Boyd. 2005. Isolation of sterol-resistant Chinese hamster ovary cells with genetic deficiencies in both Insig-1 and Insig-2. *J. Biol. Chem.* **280:** 25242–25249.
20. Goldstein, J. L., S. K. Basu, and M. S. Brown. 1983. Receptor-mediated endocytosis of low-density lipoprotein in cultured cells. *Methods Enzymol.* **98:** 241–260.
21. Brown, M. S., J. R. Faust, and J. L. Goldstein. 1978. Induction of 3-hydroxy-3-methylglutaryl coenzyme A reductase activity in human fibroblasts incubated with compactin (ML-236B), a competitive inhibitor of the reductase. *J. Biol. Chem.* **253:** 1121–1128.
22. DeBose-Boyd, R. A., M. S. Brown, W. P. Li, A. Nohturfft, J. L. Goldstein, and P. J. Espenshade. 1999. Transport-dependent prote-

olysis of SREBP: relocation of site-1 protease from Golgi to ER obviates the need for SREBP transport to Golgi. *Cell.* **99:** 703–712.
23. Metherall, J. E., J. L. Goldstein, K. L. Luskey, and M. S. Brown. 1989. Loss of transcriptional repression of three sterol-regulated genes in mutant hamster cells. *J. Biol. Chem.* **264:** 15634–15641.
24. Yang, J., R. Sato, J. L. Goldstein, and M. S. Brown. 1994. Sterol-resistant transcription in CHO cells caused by gene rearrangement that truncates SREBP-2. *Genes Dev.* **8:** 1910–1919.
25. Rawson, R. B., R. DeBose-Boyd, J. L. Goldstein, and M. S. Brown. 1999. Failure to cleave sterol regulatory element-binding proteins (SREBPs) causes cholesterol auxotrophy in Chinese hamster ovary cells with genetic absence of SREBP cleavage-activating protein. *J. Biol. Chem.* **274:** 28549–28556.
26. Yang, J., M. S. Brown, Y. K. Ho, and J. L. Goldstein. 1995. Three different rearrangements in a single intron truncate sterol regulatory element binding protein-2 and produce sterol-resistant phenotype in three cell lines. Role of introns in protein evolution. *J. Biol. Chem.* **270:** 12152–12161.
27. Liu, P., Y. Ying, Y. Zhao, D. I. Mundy, M. Zhu, and R. G. Anderson. 2004. Chinese hamster ovary K2 cell lipid droplets appear to be metabolic organelles involved in membrane traffic. *J. Biol. Chem.* **279:** 3787–3792.
28. Liang, G., J. Yang, J. D. Horton, R. E. Hammer, J. L. Goldstein, and M. S. Brown. 2002. Diminished hepatic response to fasting/refeeding and liver X receptor agonists in mice with selective deficiency of sterol regulatory element-binding protein-1c. *J. Biol. Chem.* **277:** 9520–9528.
29. Martin, S., and R. G. Parton. 2005. Caveolin, cholesterol, and lipid bodies. *Semin. Cell Dev. Biol.* **16:** 163–174.
30. Chin, D. J., K. L. Luskey, R. G. Anderson, J. R. Faust, J. L. Goldstein, and M. S. Brown. 1982. Appearance of crystalloid endoplasmic reticulum in compactin-resistant Chinese hamster cells with a 500-fold increase in 3-hydroxy-3-methylglutaryl-coenzyme A reductase. *Proc. Natl. Acad. Sci. USA.* **79:** 1185–1189.
31. Luskey, K. L., J. R. Faust, D. J. Chin, M. S. Brown, and J. L. Goldstein. 1983. Amplification of the gene for 3-hydroxy-3-methylglutaryl coenzyme A reductase, but not for the 53-kDa protein, in UT-1 cells. *J. Biol. Chem.* **258:** 8462–8469.
32. Song, B. L., N. B. Javitt, and R. A. DeBose-Boyd. 2005. Insig-mediated degradation of HMG CoA reductase stimulated by lanosterol, an intermediate in the synthesis of cholesterol. *Cell Metab.* **1:** 179–189.
33. Spence, J. T., and J. L. Gaylor. 1977. Investigation of regulation of microsomal hydroxymethylglutaryl coenzyme A reductase and methyl sterol oxidase of cholesterol biosynthesis. *J. Biol. Chem.* **252:** 5852–5858.
34. Williams, M. T., J. L. Gaylor, and H. P. Morris. 1977. Investigation of the rate-determining microsomal reaction of cholesterol biosynthesis from lanosterol in Morris hepatomas and liver. *Cancer Res.* **37:** 1377–1383.
35. Goldstein, J. L., R. B. Rawson, and M. S. Brown. 2002. Mutant mammalian cells as tools to delineate the sterol regulatory element-binding protein pathway for feedback regulation of lipid synthesis. *Arch. Biochem. Biophys.* **397:** 139–148.